PROCESSING AND IMAGING SIMULATED ULTRASONIC B-SCANS OF CONCRETE

VERARBEITUNG UND ABBILDUNG SIMULIERTER ULTRASCHALL B-SCANS VON BETON

LE TRAITEMENT ET LA FORMATION IMAGE DES B-SCANS ULTRASONIQUE SIMULE EN BETON

Eberhard Burr, Kai-Uwe Vieth, Sergei A. Shapiro

SUMMARY

Simulating ultrasonic experiments on concrete and processing the data gained in these simulations is a useful tool in nondestructive testing. The supplied data enables us to get a better understanding of the different scattering processes in the model. These synthetic datasets are also applicable for testing different processing schemes. Here, two new features are introduced for the processing of the data before or after using a SAFT-algorithm [Langenberg et al., 1993] for imaging. They both take into account that the main reflections get disturbed by the scattering effects of small air-inclusions in concrete. There are also some resuming thoughts on improvement of imaging algorithms by extending the experiments and the data accumulation to offset dependent data.

ZUSAMMENFASSUNG

Die Simulation von Ultraschallexperimenten an Beton und das Verarbeiten der dadurch gewonnenen Daten ist in der zerstörungsfreien Prüfung äusserst nützlich. Es ergibt sich dadurch die Möglichkeit einen Einblick in die Streuvorgänge im Modell zu bekommen. Desweiteren eignen sich die synthetischen Daten zum Testen verschiedener Processing-Verfahren. Das Abbilden (Imaging) wird mit Hilfe des SAFT-Algorithmus [Langenberg et al., 1993] durchgeführt. In diesem Artikel sollen zwei neue Features vorgestellt werden, welche berücksichtigen, daß die Daten durch die vielen kleinen

Lufteinschlüsse im Beton in hohem Maße verrauscht sind. Ausserdem werden noch einige Vorschläge zur Verbesserung der Imaging-Ergebnisse, durch Berücksichtigung von offset-abhängigen Daten, gemacht.

RESUME

La simulation des expériences ultrasoniques sur béton et le traitement des données gagnées dans ses simulations est en tres utile essai nondestructif. Il y a la possibilité pour obtenir une perspicacité de des procédés de dispersion dans le modèle et aussi il y a la possibilité de recevoir un ensemble de données relativement facile d'essai pour différents arrangements de traitement. Voici deux nouveaux dispositifs présentés pour le prétraitement des données avant ou après l'utilisation d'un SAFT-algorithme [Langenberg et al., 1993] pour la formation image. Ils tous les deux tiennent compte que les réflexions principales obtiennent troublées par les effets de dispersion des petites inclusions d'air en béton. Également il y a quelques pensées de reprioe sur l'amélioration des formations images-algorithme en étendant les expériences et l'accumulation aux données excentrer-dépendantes.

KEYWORDS: synthetic ultrasonic experiments, imaging, processing

INTRODUCTION

Data of ultrasonic experiments on conrete have a very complex and problematic structure. Even extremely accurate FD-simulations cannot represent all the effects to be taken into account when dealing with such a complicated medium. The output of such simulations lacks the influence of the receiver characteristics (coupling, resonance frequencies, diameter). Beside the scattering noise produced by small air inclusions, there is no experimental noise. Real experiments always are 3D-experiments where out of plane reflections occur. Of course, this side effect is not considered when working with 2D-simulations. Even the data of a simple synthetic 2D-configuration is hard to handle when one creates an image of the inner structure of the investigated concrete in order to detect cracks and flaws in a given depth. Because real data are always of minor quality compared to synthetic data, our synthetic data, strongly dominated by air

inclusion scattering are a good experimental environment to test processing- and imaging-algorithms before applying them to real ultrasonic B-Scans.

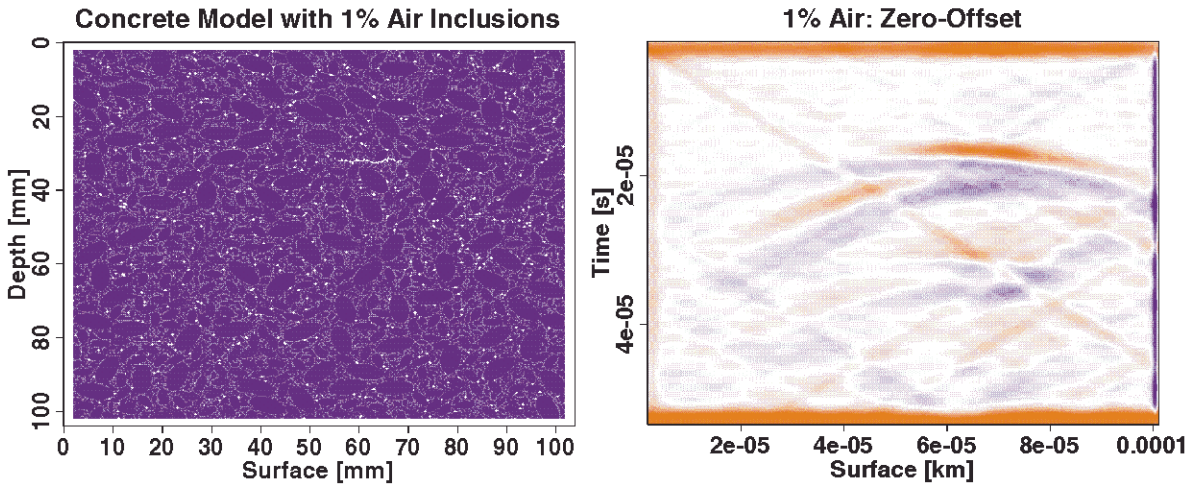

Fig. 1: *A Model with 1% air-inclusions and its B-Scan recorded at the surface.*

SIMULATION AND PROCESSING

To test the new processing features the same simulation models and the same synthetic datasets as in the last article [Burr et al., 1997] were used. The concrete model existed of a two-dimensional 10cm*10cm block with ellipses of different sizes, which represent the stuffing material and with very small ellipses which represent the air-inclusions that are responsible for the high scattering noise in the data. All ellipses are randomly placed and orientated. The percentage of the air-inclusion is varried from one percent to four percent to gain datasets with a different degree of difficulty. A small flaw with a fractal shape is placed horizontally in three centimeters depth and with a lateral extension of two centimeters. In the model with four percent air-inclusions the flaw is placed a bit diogonally.

A plane wave is propagated through the medium and the reflections are recorded at every of the 500 gridpoints at the surface of the model (Fig. 1 and 2). The received B-Scans are processed in different ways.

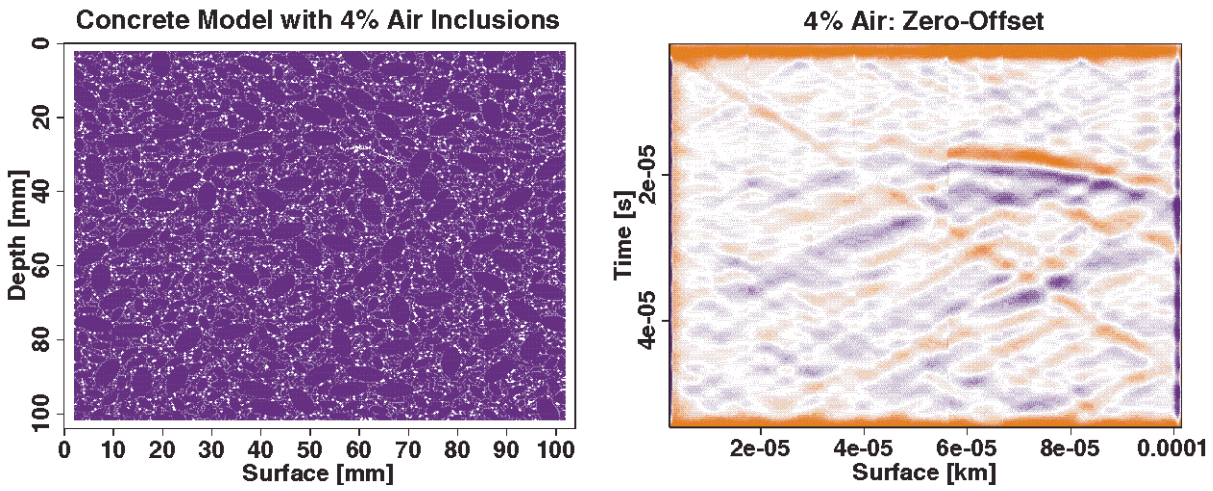

Fig. 2: *A model with 4% air inclusions and its B-Scan.*

The imaging process is based on the SAFT-algorithm which here presupposes a homogenous velocity of 4000 m/s. Because of the stuffing and air-inclusions concrete is treated as a random medium. Therefore, a randomizer is brought into action while building a model. The random medium gives rise to talk about an effective velocity rather than a homogenous velocity.

The image is more robust and interpretation is easier and more obvious when one calculates the envelope after imaging. The envelope or instantanous amplitude represents the absolute value of the analytical or complex signal [Buttkus, 1991], respectively. This processing step was first used in geophysics for yielding an image from seismic reflection experiments in strongly fractured cristalline rocks [Simon, 1998]. The Envelope procedure avoids destructive interference of amplitudes due to imperfect velocity estimations applied in the imaging algorithm.

A coherency criteria is also implemented into the imaging algorithm. It is called semblance [Taner and Köhler, 1996] and corresponds to the normalized ratio of the output to the input energy. An exact phase alignment along the summed trajectory yields the maximum whereas white noise the minimum value. The values are in the intervall $0 \le S \le 1$.

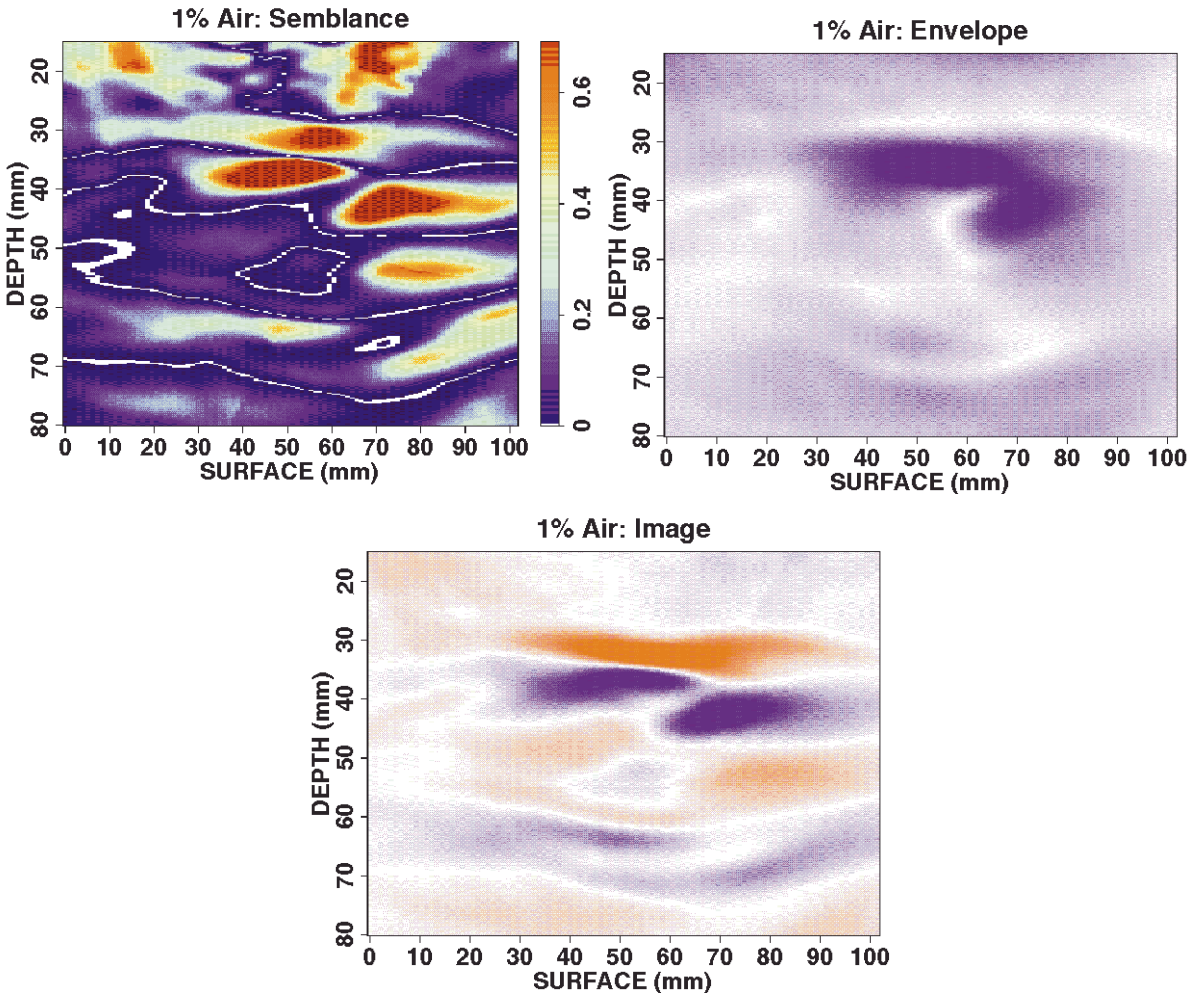

Fig. 3: *Different images out of the B-Scan with 1% air inclusions*

After the preprocessing the SAFT-algorithm generates an image of the dataset. Every imagepoint is associated with the sum of amplitudes lying on a parabolic shaped trajectory in the data space (Using a point source would result in summing along a diffraction hyperbola.).

With respect to the results of [Burr et al., 1997] the imaging algorithm has been improved by implementing a weighing factor which considers two physical aspects. The first one is called 'geometrical spreading factor' or 'spherical divergence', respectively. The intensity, ie. the quantity of energy that flows through a unit area normal to the direction of wave propagation in unit time, is inversely proportional to the distance between source and wavefront. therefore,

we can write $\frac{I_2}{I_1} = (\frac{R_2}{R_1})^M$ where M = 0, 1, or 2 according as the wave is plane, cylindrical, or spherical. I_1, I_2, R_1 and R_2 are the intensities and radii of the wavefront at time 1 and 2. The second aspect takes into account that an incident wave forms an angle φ with the normal of the surface and receiver, respectively. this obliquity factor considers that only the cosine of the amplitude has been registered.

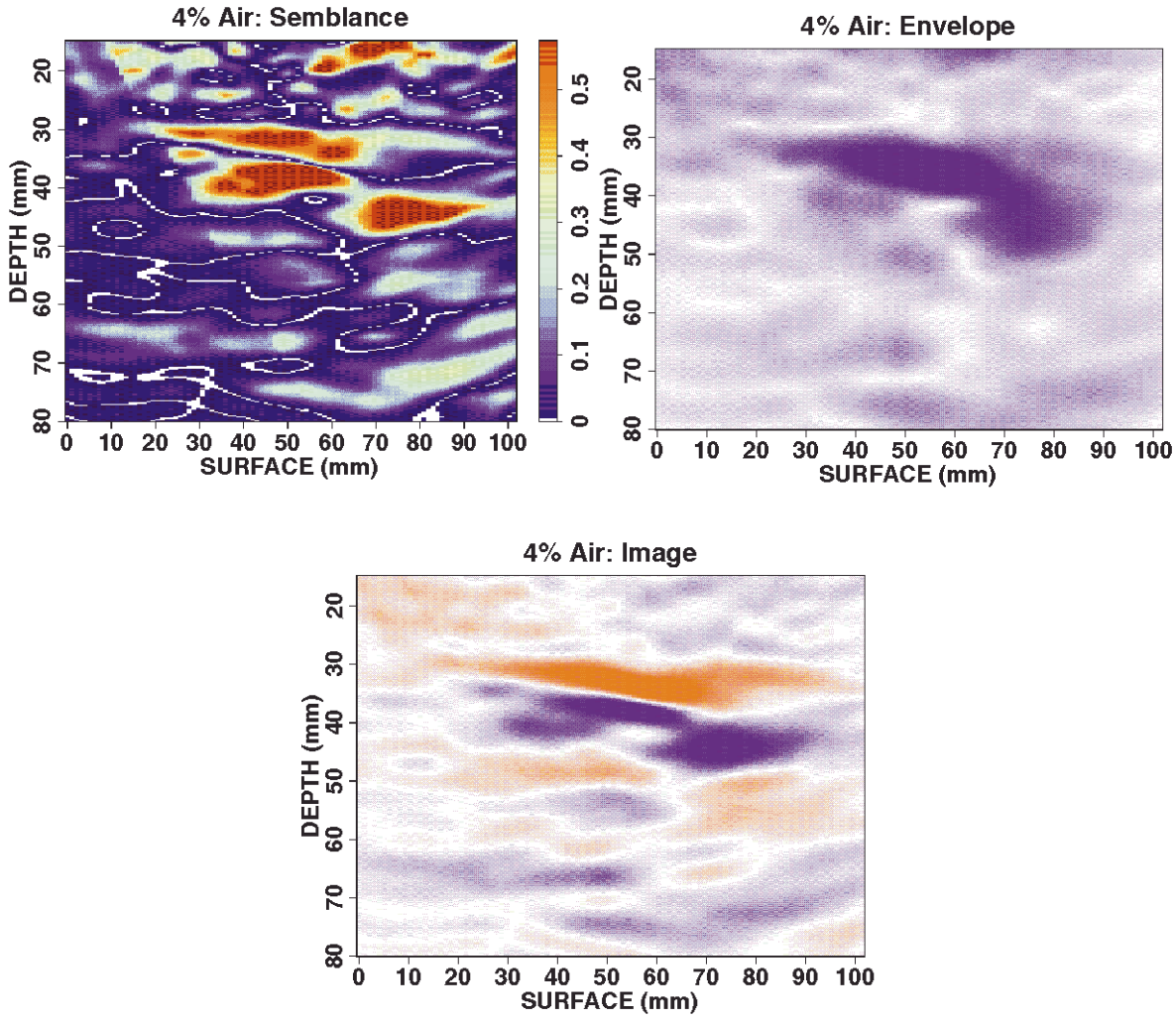

Fig. 4: *Different images out of the B-Scan of concrete with 4% air inclusions.*

RESULTS

In the first simulation there was used one percent air-inclusions in the concrete model (Fig. 1). The second example is a bit more complicated with four percent air-inclusions (Fig. 2). Both new features were tested individually at the two synthetic datasets. The data resulting from these different processing schemes is imaged with the SAFT-algorithm and compared with the unprocessed example. So we gain an envelope-image, a semblance-image and an unprocessed image for every synthetic dataset.

In figure 3 the semblance-image brings a small improvement for the detection of the flaw. The lateral extend of the flaw is better than in the unprocessed image but not as good as in the envelope-image. Also the image of the flaw is shifted to the left in comparison with the model. Every artifact in the unprocessed image has a counterpart in the semblance-image. So the depressing of multiple reflections and other artifacts, for example due to shear and surface waves or sizeeffects, is not possible with this processing scheme. But it is expected to bring better results if the signal to noise ratio is lower, for example in medias with weak scattering inhomogenities.

As it is seen in Fig. 3 and Fig. 4, there is a much higher dynamic range of the amplitudes that survives the imaging process, when the envelopes are formed after the use of the SAFT-algorithm. In comparison with the other images, the envelope-image is the best without artifacts, the flaw is always placed in the right area and its inclination in comparison to the surface is correct. In the 4% model (Fig. 2) the flaw was a bit more bent and in the 4% envelope-image (Fig. 4) this difference is seen very well. The envelope-images have also the highest contrast between flaw and environment and the best lateral dissolution. The only thing to critisize is the unsharp profile of the flaw, but the upper edge in the image is always representing the correct depth.

In every image there is an artifact latarally under the right side of the image of the flaw. This is due to the energy reflected at the flaw not directly back to the surface but with another reflection at the right side of the model. Maybe the imaging-algorithm should take these reflections into account and when the

parabola reaches the edge of the data-space, the summation shouldn't be stopped. There is the possibility for image-points near the sides of the image-array to mirror the branch of the parabola reaching the edge back into the data-space and to continue the sumation. This would be an easy task for such simple shaped images like in our example and this step would eliminate the last artifact out of the envelope-image.

CONCLUSIONS

Because there is further a unsatisfactorily yield due to reduced resolution there should be thought about a recording of more complex datasets then only B-Scans. If there are some other possibilitys to illuminate the investigated body not only with a transducer but with different source-receiver-constellations the dataset would have more information but it would be also more complex to image and more expensive to measure.

In these simulations there were used perfect pointlike receivers. In real experiments there is always the problem: Take a receiver with a small diameter and it has a reduced sensitivity and is only available for lower frequencies. Take a receiver with a long diameter than you have a higher sensitivity but you average out all the informations in the high frequencies. It would be a large improvement if averaging would only be done by the processing- or imaging-algorithm and not by the receiver.

So the main problem in ultrasonics is how to get as much information as possible into the data and how to extract the necessary informations for the image. These two processing schemes introduced in this article are a small step in the right direction. Mainly the formation of envelopes as a processing step gives really a rough estimate of the orientation and placement of the flaw.

The used programe and its features has also being designed for interactive use under Windows and this version will be necessary as soon as real

experiments on concrete will take place in the innovative research group of the FMPA.

ACKNOWLEDGEMENTS

We gratefully acknowledge funding of our work by the Deutsche Forschungs Gemeinschaft (DFG) in part A6 and C4 of the collaborative research center 381 'Charakterisierung des Schädigungsverlaufes in Faserverbundwerkstoffen mittels zertörungsfreier Prüfung'.

REFERENCES

BURR, E., GOLD, N., GROSSE, C., REINHARDT, H.-W. (1997*): Simulation of Ultrasonic Flaw-Detection in Concrete with a different Percentage of Air Inclusions,* Otto-Graf-Journal. Vol. 8. P. 19-29.

BURR, E., GROSSE, C., REINHARDT, H.-W. (1997): *Application of a modified SAFT-Algorithm on Synthetic B-Scans of Coarse Grained Materials,* Otto-Graf-Journal. Vol. 8. P. 30-44.

BUTTKUS, E. (1991): *Spektralanalyse und Filtertheorie in der angewandten Geophysik*, Springer Verlag, Berlin.

LANGENBERG, K.-J.,FELLINGER, P., MARKLEIN, R., ZANGER, P., MAYER, K., KREUTTER, T., (1993): *Inverse Methods and Imaging*. P. 317-398. Out of *Evaluation of Masterials and structures by quantitative ultrasonics* from J.D. ACHENBACH. Springer Verlag, Wien New York.

SIMON, M. (1998): *AVO analysis by offset-limited prestack migrations of crustal seismic data*. Tectonophysics 286 (1998) P. 143-153.

TANER, KÖHLER (1996): *Velocity spectradigital computer deviation and applications of velocity functions*. Geophysics V.34, P.859-881.